PHYSICAL REVIEW B **93**, 220406(R) (2016)

Exchange interactions of magnetic surfaces below two-dimensional materials

Rico Friedrich,* Vasile Caciuc, Nicolae Atodiresei,† and Stefan Blügel
Peter Grünberg Institut (PGI-1) and Institute for Advanced Simulation (IAS-1), Forschungszentrum Jülich and JARA, D-52425 Jülich, Germany

(Received 7 April 2016; revised manuscript received 6 June 2016; published 22 June 2016)

In this theoretical investigation we demonstrate that the adsorption of spatially extended two-dimensional (2D) π systems such as graphene and hexagonal boron nitride on the ferromagnetic fcc Co(111) surface leads to a specific behavior of the in-plane and interlayer Co-Co magnetic exchange interactions. More specifically, for both systems the magnetic exchange coupling within the first Co layer is enhanced, while the one between the first and the second Co layer is not modified, in contrast to the magnetic interlayer softening induced by organic molecules. Importantly, the in-plane magnetic hardening effect is mainly due to the hybridization between the p_z states of the 2D π system and the d states of the Co surface.

DOI: 10.1103/PhysRevB.93.220406

The ability to prepare high-quality two-dimensional (2D) materials on semiconductor and metal surfaces has opened the path to investigate a variety of fundamental physical properties of such systems, of which graphene [1] is the most prominent example. Among these are the study of a two-dimensional gas of massless Dirac fermions [2], the observation of the quantum Hall effect and Berry phase [3], the prediction of a quantum spin Hall effect [4], and perfect spin filters [5], but also many other interesting physical properties that are reviewed in detail in Refs. [6,7].

With the prospect of future spintronics applications, of special interest are the studies of graphene on transition-metal substrates such as Fe, Co, Ni, and Au that have been the focus of several recent experimental and theoretical investigations [8–16]. For instance, the weak hybridization between the graphene π orbitals and the d states of the Au atoms in the case of a graphene-Au-Ni(111) system induces an experimentally measurable Rashba effect into the graphene electronic structure [8,11]. Furthermore, the adsorption of graphene on more reactive substrates such as Co(0001), Co/Ir(111), and Fe/Ir(111) leads to a strong π-d hybridization and consequently to the creation of a new hybrid material whose properties can be considerably different than those of the separated components [9,10,14,17].

In this Rapid Communication we explore how the adsorption of spatially extended two-dimensional (2D) π systems such as graphene and hexagonal boron nitride (hBN) on fcc Co(111) modifies the magnetic properties of this substrate. It is important to note that finite-size small π-conjugated systems such as molecules adsorbed on ferromagnetic surfaces can significantly change the magnetic properties of the substrate. For example, experimentally and theoretically it was shown that the deposition of phenalenyl-like molecules on a Co(111) surface reduces the interlayer magnetic exchange coupling between the first and second Co layer, known as interlayer magnetic softening [18,19]. Furthermore, theoretical simulations demonstrated that the paracyclophane molecule chemisorbed on a Fe/W(110) surface locally enhances the magnetic exchange coupling of the metal atoms below the molecule (in-plane magnetic hardening) that practically leads to an enhanced coercive field for the hybrid molecule-surface system compared to the clean surface [20]. In particular, this magnetic hardening effect has been directly measured in recent scanning tunneling microscopy (STM) experiments performed on π-conjugated systems adsorbed on a noncollinear magnetic structure. More precisely, the chemisorption of coronene molecules and graphene nanoflakes onto a 1 monolayer (ML) Fe/Ir(111) surface results in the formation of local hybrid ferromagnetic (collinear) units immersed into the noncollinear background that switch under an applied magnetic field [14]. Even more interestingly, the modification of the in-plane magnetic exchange coupling of the surface metal atoms below such π-conjugated organic molecules can be specifically controlled by employing a chemical functionalization of the adsorbed molecule. As a direct consequence, the coercive field of such hybrid molecule-magnetic surface systems can be precisely tailored over a wide range [21]. To summarize, in a general picture, these *ab initio* studies revealed that the hardening/softening of the magnetic exchange coupling due to molecular adsorption implies an interplay between (i) an adsorbate-substrate hybridization effect describing the hybridization of the molecular electronic states with the substrate ones and (ii) a geometrical effect defined by the re-hybridization between the surface atoms' d states due to structural changes of the surface induced by the molecular adsorption [19–21].

The main goal of our first-principles calculations in this work here is to determine how the extended π systems differ from the finite molecular ones and how they can be employed to engineer the strength of the exchange interactions of a magnetic surface, exemplified by Co(111), via the adsorption of specific 2D systems. For this purpose we have chosen to investigate two extended π systems described by a similar honeycomb lattice containing two atoms per primitive unit cell but with a different electronic structure: (i) graphene, a "zero-gap insulator" with a linear dispersion at the band crossings at the K and K' points of the 2D Brillouin zone, a property of the energy dispersion known as a Dirac cone [6], and (ii) hexagonal boron nitride (hBN), an atomically thin film that is an insulating material with an experimental band gap of 5.5 eV [22]. As a characteristic that is common to both materials, the occupied and unoccupied bands close to the Fermi energy, that determine the interaction of the 2D

*r.friedrich@fz-juelich.de
†n.atodiresei@fz-juelich.de

material with the surface, have bonding π and antibonding π^* character. Our results show that after adsorption both extended π systems modify the magnetism of the underlying substrate in a similar way, i.e., induce an in-plane hardening of the magnetic exchange interactions $J_\parallel$ within the first Co layer. This finding is demonstrated to be qualitatively similar to the case of a Co monolayer intercalated below graphene on Ir(111). However, surprisingly, the adsorption of graphene and hBN on Co(111) does not modify the interlayer exchange coupling constant $J_\perp$ between the first and the second Co layer. A careful analysis of the electronic structure of the hybrid π-metal-surface interfaces considered in our study reveals that the in-plane hardening is the result of a strong p_z-d hybridization between the 2D material film (i.e., graphene or hBN) and the first layer metal states of the substrate. In consequence, this in-plane hardening of the exchange coupling constants is a 2D material-induced hybridization effect [20,21].

The spin-polarized electronic structure calculations were carried out in the framework of density functional theory (DFT) [23,24] using the VASP program [25,26]. In addition, pseudopotentials generated by the projector augmented-wave (PAW) method [27] were used as constructed for the exchange-correlation functional of Perdew, Burke, and Ernzerhof (PBE) [28]. Throughout all calculations a plane wave cutoff of 500 eV was used and a 2D k-point set of 32×32 was applied. All structures were relaxed until the forces were smaller than 1 meV/Å. As Co is well known to exhibit strong correlation effects [29], the DFT+U formalism [30] has been applied for all calculations in the rotational invariant form [31] with an effective Hubbard interaction parameter $U_{\text{eff}} = 3$ eV, consistent with previous calculations [18,29].

The supercell incorporated seven Co layers in fcc stacking, each represented by a 1×1 in-plane unit cell containing one Co atom and one layer of 2D material incorporating two atoms. This is consistent with the common procedure of previous investigations in Refs. [5,13,17,32] to make the 2D material commensurate with the underlying substrate as their lattice parameters match almost perfectly [5,13,33] (at least by $\approx 98\%$). The vacuum in a direction perpendicular to the surface plane was modeled by a region set to a width of 18 Å to avoid the interaction between the periodic images.

To identify the ground-state adsorption geometries, we took into account three different possibilities to place the two layer atoms into high symmetry positions in the unit cell (see Fig. 1 in the Supplemental Material [34] for a visualization of these structures). All systems were structurally optimized with the experimental lattice constant of 3.545 Å of fcc Co [35]. During the geometry optimization, the upper four Co layers and the coordinates of the 2D materials were allowed to relax. Focusing on the structural optimization, the rev-vdW-DF2 functional [36–41] was used in order to properly include the nonlocal correlation effects responsible for the long-range van der Waals (vdW) interactions. The exchange coupling constants were determined from total energy differences between anti- and ferromagnetic configurations for which the PBE+U functional provides reliable results.

As a result of the structural optimization of the different graphene/hBN-surface geometries, it is found that the lowest energy is obtained for the top-hcp geometry (i.e., one C/N atom on top of a Co atom and the other C/B atom on a hcp hollow site between three Co atoms) [see Figs. 1(a) and 1(b)], consistent with previous investigations [42]. The adsorption energies for the top-hcp geometries are included in Table I. This adsorption geometry is favored by at least 0.1 eV in both cases (a comparison of the adsorption energies for both systems is shown in Table I of the Supplemental Material). Overall, the magnitude of the adsorption energies suggests that both systems bind to the Co(111) surface by a weak chemisorption type bonding mechanism, as was also suggested in Ref. [42] for graphene on Co(111).

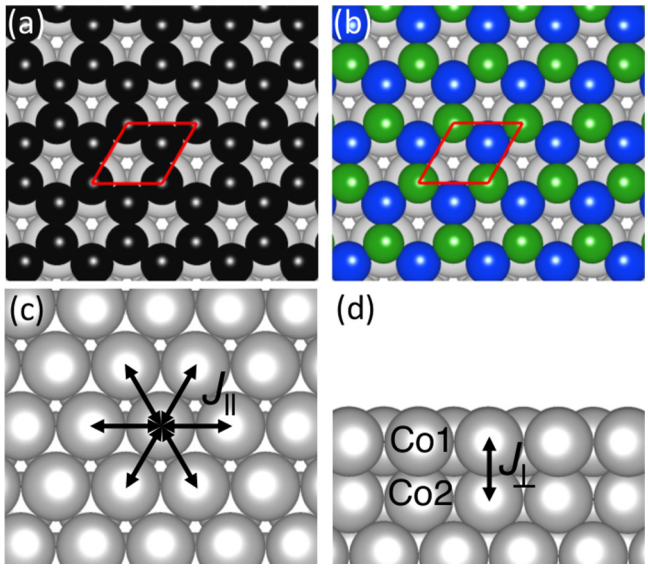

FIG. 1. Top-hcp geometry for graphene (a) and hBN (b) adsorbed on Co(111). The unit cell of each system is marked by the red parallelogram. Color code: gray=Co, black=C, blue=B, green=N. Assignment of the in-plane $J_\parallel$ (c) and interlayer $J_\perp$ (d) exchange coupling constants of the Co(111) surface.

Moreover, the adsorption of graphene and hBN modifies the magnetic moments of the first Co layer to a significant extent, as presented in Table I. The magnetic moment of the surface Co1 atom directly bound to the extended π systems is reduced from the pristine surface value of $1.95\mu_B$ to about $1.8\mu_B$ caused by hybridization between the p_z-atomic-like states of graphene and hBN with the out-of-plane $d_{z^2,xz,yz}$ states of the Co(111) surface. On the contrary, the moment of the subsurface Co2 atom is practically not affected (only changed by $0.01\mu_B$) [43], indicating that the influence of the 2D system is essentially confined to the first surface layer.

Now we turn to the procedure of how to evaluate the in-plane and interlayer magnetic exchange coupling constants J between the Co atoms of the substrate. We describe the exchange coupling between the magnetic moments of the Co atoms by an effective Heisenberg Hamiltonian, taking into account only the nearest-neighbor interactions, as already applied previously by us [14,18–21], $\hat{H} = -\sum_{i>j} J_{ij}\mathbf{m}_i\mathbf{m}_j$, where $\mathbf{m}_i$ and $\mathbf{m}_j$ stand for the magnetic moments of the atoms i and j, respectively. Consequently, the energy difference between a ferromagnetic and an antiferromagnetic configuration can be expressed as $E_{\text{FM}} - E_{\text{AFM}} = -2\sum_n N_n J_n m_n m'_n$,

TABLE I. Evaluated adsorption energies E_{ads} per unit cell for graphene and hBN on Co(111). Note that the adsorption energy is defined as $E_{ads} = -[E_{sys} - (E_{subst} + E_{2D})]$, where E_{sys} stands for the total energy of the hybrid 2D material-surface system, E_{subst} indicates the total energy of the substrate, and E_{2D} represents the total energy of the freestanding layer of graphene or hBN, respectively. The Co-Co and C/N/B-Co distances are given in Å, the magnetic moments of the cobalt atoms in the first (Co1) and second (Co2) surface layer are given in μ_B, and the theoretical exchange coupling constants for the 2D material-surface systems and the clean surface geometries induced by the 2D systems are specified in meV per pair.

					Magnetic moments		With 2D material		Induced geometry	
System/surface	E_{ads} (eV)	Co1-Co2	C_{top} (N)-Co1	C_{hcp} (B)-Co1	Co1	Co2	$J_\parallel$	$J_\perp$	$J_\parallel$	$J_\perp$
Clean surface		2.45			1.95	1.87	32.0	62.2	32.0	62.2
Graphene	0.43	2.48	2.09	2.52	1.81	1.87	85.0	61.6	32.8	56.4
hBN	0.38	2.46	2.15	2.50	1.83	1.88	68.2	62.8	31.1	59.8

where m_n and m'_n are the magnetic moments of the interacting Co atoms and N_n stands for the number of equivalent neighbors of sort n. Using this equation for a suitably chosen set of antiferromagnetic configurations, a linear system of equations can be obtained and used to calculate the exchange coupling parameters J.

As shown in Figs. 1(c) and 1(d), two different types of coupling constants are modified by the adsorption of the π-electron systems graphene and hBN, namely, the in-plane exchange coupling constant $J_\parallel$ describing the coupling between the Co atoms within the first layer and the interlayer exchange coupling parameter $J_\perp$ describing the coupling between the first and second Co layer. To evaluate the in-plane exchange parameter $J_\parallel$, a 2×2 unit cell was chosen which allows one to calculate a row-wise antiferromagnetic state of the first layer moments.

The calculated exchange coupling constants obtained by using the above-mentioned method are reported in Table I. We note that our calculated exchange coupling constant for bulk fcc Co is $J_{bulk} = 24.4$ meV (8.0 meV/μ_B^2) [44], which is in reasonable agreement with the values of 27.64 meV and 8.54 meV/μ_B^2 given in Refs. [45] and [18], respectively [46]. As a general feature, a strong enhancement of the in-plane exchange coupling constant $J_\parallel$ from 32.0 meV for the clean surface to 85.0 and 68.2 meV due to the adsorption of graphene and hBN on the Co(111) surface is found. We note that the clean surface exchange coupling constant is close to the bulk value [45,46].

To compare with the case of a single Co layer, we performed additional *ab initio* calculations and evaluated the in-plane exchange coupling constants for a Co monolayer intercalated between a (10×10) graphene on a (9×9) Ir(111) substrate [9]. These simulations revealed that at those regions where graphene forms strong chemical bonds with the Co atoms, a large in-plane hardening of the coupling constants occurs, i.e., the coupling constants increase [see the fcc and hcp chemisorbed sites in Fig. 1(d) in Ref. [9]]. The corresponding theoretical $J_{fcc} = 41.5$ meV and $J_{hcp} = 37.6$ meV are almost one order of magnitude larger than that evaluated at the weakly interacting (physisorbed) top site $J_{top} = 4.1$ meV, the latter value being practically identical with the exchange coupling of 4.0 meV evaluated for the clean Co layer on Ir(111). A direct comparison with the Co(111) surface reveals that the in-plane exchange coupling constant of the clean Co monolayer on Ir(111) is significantly smaller (i.e., 32 vs 4 meV). Besides this, in both cases the chemisorbed graphene layer induces a significant increase of the in-plane J and the magnitude of this enhancement is more pronounced in the case of Co(111) than for the Co/Ir(111) system.

On the other hand, we would like to emphasize that the direct consequence of the increased in-plane exchange coupling constant at the chemisorbed sites represents a magnetic hardening effect. This is clearly evidenced by the opening of the hysteresis loop measured experimentally for the graphene/Co/Ir(111) system [9] as compared to the clean Co/Ir(111) substrate [47]. At this point it is important to mention that a similar behavior was observed for the graphene/Fe/Ir(111) system [10,48] and also for an Fe/Ir(111) substrate upon adsorption of coronene molecules and graphene nanoflakes [14]. On this basis we suggest that this magnetic hardening effect can also be experimentally measured for graphene and hBN adsorbed on the Co(111) substrate.

As already discussed in several previous studies [14,20], the in-plane hardening of the J's induced by a π-electron system on a magnetic surface is a direct consequence of the strong hybridization between the out-of-plane d states of the magnetic substrate and the p_z-atomic-like ones of graphene (hBN), a contribution denoted in the following as p_z-d hybridization. More precisely, a strong 2D material-substrate hybridization process can be clearly identified from the analysis of the spin-polarized projected density of states (SP-PDOS) obtained for all d states of Co1 [see Fig. 2(a)] and that calculated for the p_z-atomic-like states of the graphene and hBN [see Figs. 2(b) and 2(c), respectively]. In particular, the Co1 SP-PDOS of the hybrid systems depicted in Fig. 2(a) is strongly modified when compared to the corresponding SP-PDOS of the clean surface atom. This observation indicates a significant hybridization with the p_z states at the 2D material site, as clearly illustrated in Figs. 2(b) and 2(c). We also note that the SP-PDOS of the p_x and p_y states shows practically no hybridization with the surface d states, implying that indeed the p_z-d hybridization is the dominant mechanism of the in-plane hardening of the magnetic exchange interactions. In addition, the SP-PDOS of the d states for the second Co layer (not shown) is considerably less modified by the adsorption of the π-electron systems than in case of the Co1 atom. This analysis clearly demonstrates that the graphene and hBN adsorption directly changes

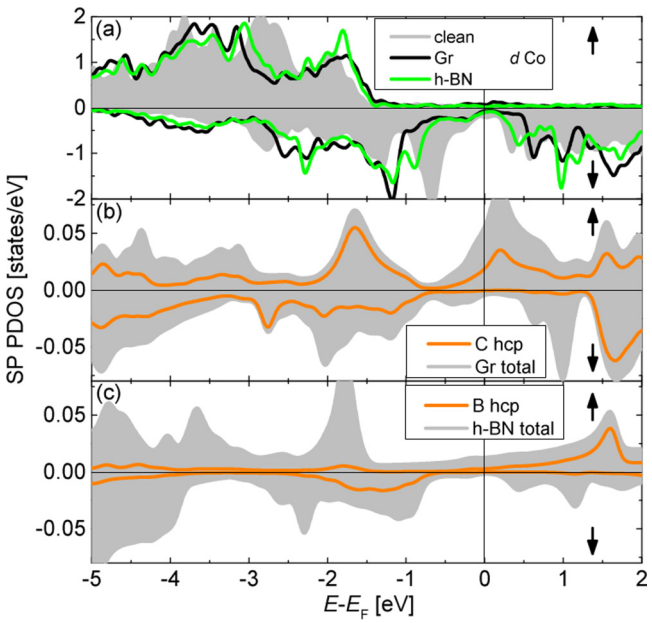

FIG. 2. (a) SP-PDOS for all d states of Co1 for the clean surface and for graphene (Gr) and hBN adsorbed on the Co(111) surface. SP-PDOS for the π states of (b) Gr and (c) hBN chemisorbed on Co(111). Note that the p_z states of graphene and hBN are significantly hybridized with the d states of the Co substrate. The p_z contributions of the C and B atoms in the hollow hcp sites are also presented.

only the electronic and magnetic properties of the first Co layer.

To emphasize the importance of this fact, we have re-calculated the exchange coupling constants for the relaxed geometries of the hybrid systems but with the 2D materials removed so that the contribution of the geometrical changes of the substrate induced by graphene and hBN adsorption can be disentangled. The resulting exchange coupling constants for the 2D material-induced surface geometries are reported in Table I. From these values it can be clearly seen that without the presence of the graphene or hBN, the same surface geometry does not significantly change the in-plane magnetic exchange coupling constant $J_{\parallel}$ of the clean surface. This observation unequivocally demonstrates that the 2D material-surface hybridization (i.e., p_z-d hybridization effect) is essential to induce the in-plane hardening of the magnetic exchange interactions.

Interestingly, the calculated values for the interlayer exchange coupling constant $J_{\perp}$ reported in Table I do not indicate any clear hardening or softening of the interlayer magnetic interactions. Notably, this outcome of our *ab initio* simulations is in contrast to the previous studies for spatially finite molecular π systems adsorbed on magnetic substrates. More precisely, the zinc methyl phenalenyl molecule chemisorbed on the Co(111) surface [18] but also the dioxan and dioxin molecules adsorbed on 2 ML Fe/W(110) [19] give rise to an interlayer softening of the calculated exchange coupling constants $J_{\perp}$ due to a skyhook effect, i.e., the Co/Fe surface atoms under the molecules are slightly lifted from the magnetic substrates due to the Co/Fe-molecule interaction.

As a final note, it is important to mention that the 2D π systems graphene and hBN on Co(111) acquire no net magnetic moment. Nevertheless, as depicted in Figs. 2(b) and 2(c), they exhibit a net spin polarization in a given energy interval with respect to the Fermi energy of the graphene(hBN)/Co(111) system, as also shown for several π molecules adsorbed on magnetic surfaces [49,50].

To conclude, our first-principles study reveals that the interaction of an extended 2D π-electron system such as graphene and hBN with a ferromagnetic Co(111) substrate leads to an in-plane hardening of the magnetic exchange interactions. In this respect our calculations indicate that the 2D material-Co(111) system exhibits a stronger in-plane Co exchange interaction as compared to the clean Co(111) surface, and this in-plane enhancement of the exchange coupling constants is essentially due to the hybridization between the 2D materials p_z- and the substrate d-electronic states (i.e., 2D material-substrate p_z-d hybridization effect). Note that a similar behavior was observed for the system graphene on Co/Ir(111). On the other hand, our calculations carried out for graphene and hBN covered Co(111) revealed no hardening or softening for the interlayer magnetic interactions in contrast to finite π-molecular systems. This implies that a spatially extended π system can be used to selectively preserve the magnetic properties of a substrate of choice [51].

Overall, our *ab initio* results clearly demonstrate the potential of the extended 2D π-electron systems to change or maintain the magnetic properties of a ferromagnetic surface. Therefore, the knowledge gained in this study can play an important role to precisely control the magnetism at the graphene/hBN-electrode contacts for a better efficiency of graphene/hBN-based spintronic devices.

The computations were performed under the auspices of the VSR at the computer JURECA and the GCS at the high-performance computer JUQUEEN operated by the JSC at the Forschungszentrum Jülich. N.A. and V.C. gratefully acknowledge financial support from the Volkswagen-Stiftung through the "Optically Controlled Spin Logic" project.

[1] K. S. Novoselov, D. Jiang, F. Schedin, T. J. Booth, V. V. Khotkevich, S. V. Morozov, and A. K. Geim, Proc. Natl. Acad. Sci. USA **102**, 10451 (2005).

[2] K. S. Novoselov, A. K. Geim, S. V. Morozov, D. Jiang, M. I. Katsnelson, I. V. Grigorieva, S. V. Dubonos, and A. A. Firsov, Nature (London) **438**, 197 (2005).

[3] Y. Zhang, Y.-W. Tan, H. L. Stormer, and P. Kim, Nature (London) **438**, 201 (2005).

[4] C. L. Kane and E. J. Mele, Phys. Rev. Lett. **95**, 226801 (2005).

[5] V. M. Karpan, G. Giovannetti, P. A. Khomyakov, M. Talanana, A. A. Starikov, M. Zwierzycki, J. van den Brink, G. Brocks, and P. J. Kelly, Phys. Rev. Lett. **99**, 176602 (2007).

[6] A. H. Castro Neto, F. Guinea, N. M. R. Peres, K. S. Novoselov, and A. K. Geim, Rev. Mod. Phys. **81**, 109 (2009).

[7] A. K. Geim and K. S. Novoselov, Nat. Mater. **6**, 183 (2007).

[8] Y. S. Dedkov, M. Fonin, U. Rüdiger, and C. Laubschat, Phys. Rev. Lett. **100**, 107602 (2008).
[9] R. Decker, J. Brede, N. Atodiresei, V. Caciuc, S. Blügel, and R. Wiesendanger, Phys. Rev. B **87**, 041403(R) (2013).
[10] R. Decker, M. Bazarnik, N. Atodiresei, V. Caciuc, S. Blügel, and R. Wiesendanger, J. Phys.: Condens. Matter **26**, 394004 (2014).
[11] D. Marchenko, A. Varykhalov, M. Scholz, G. Bihlmayer, E. Rashba, A. Rybkin, A. Shikin, and O. Rader, Nat. Commun. **3**, 1232 (2012).
[12] A. B. Shick, S. C. Hong, F. Maca, and A. I. Lichtenstein, J. Phys.: Condens. Matter **26**, 476003 (2014).
[13] G. M. Sipahi, I. Žutić, N. Atodiresei, R. K. Kawakami, and P. Lazic, J. Phys.: Condens. Matter **26**, 104204 (2014).
[14] J. Brede, N. Atodiresei, V. Caciuc, M. Bazarnik, A. Al-Zubi, S. Blügel, and R. Wiesendanger, Nat. Nanotechnol. **9**, 1018 (2014).
[15] W. Han, R. K. Kawakami, M. Gmitra, and J. Fabian, Nat. Nanotechnol. **9**, 794 (2014).
[16] D. Marchenko, A. Varykhalov, J. Sanchez-Barriga, O. Rader, C. Carbone, and G. Bihlmayer, Phys. Rev. B **91**, 235431 (2015).
[17] D. Eom, D. Prezzi, K. T. Rim, H. Zhou, M. Lefenfeld, S. Xiao, C. Nuckolls, M. S. Hybertsen, T. F. Heinz, and G. W. Flynn, Nano Lett. **9**, 2844 (2009).
[18] K. V. Raman, A. M. Kamerbeek, A. Mukherjee, N. Atodiresei, T. K. Sen, P. Lazić, V. Caciuc, R. Michel, D. Stalke, S. K. Mandal, S. Blügel, M. Münzenberg, and J. S. Moodera, Nature (London) **493**, 509 (2013).
[19] R. Friedrich, V. Caciuc, N. Atodiresei, and S. Blügel, Phys. Rev. B **92**, 195407 (2015).
[20] M. Callsen, V. Caciuc, N. Kiselev, N. Atodiresei, and S. Blügel, Phys. Rev. Lett. **111**, 106805 (2013).
[21] R. Friedrich, V. Caciuc, N. S. Kiselev, N. Atodiresei, and S. Blügel, Phys. Rev. B **91**, 115432 (2015).
[22] L. Song, L. Ci, H. Lu, P. B. Sorokin, C. Jin, J. Ni, A. G. Kvashnin, D. G. Kvashnin, J. Lou, B. I. Yakobson, and P. M. Ajayan, Nano Lett. **10**, 3209 (2010).
[23] P. Hohenberg and W. Kohn, Phys. Rev. **136**, B864 (1964).
[24] W. Kohn and L. J. Sham, Phys. Rev. **140**, A1133 (1965).
[25] G. Kresse and J. Hafner, Phys. Rev. B **49**, 14251 (1994).
[26] G. Kresse and J. Furthmüller, Phys. Rev. B **54**, 11169 (1996).
[27] P. E. Blöchl, Phys. Rev. B **50**, 17953 (1994).
[28] J. P. Perdew, K. Burke, and M. Ernzerhof, Phys. Rev. Lett. **77**, 3865 (1996).
[29] V. A. d. l. P. O'Shea, I. d. P. R. Moreira, A. Roldan, and F. Illas, J. Chem. Phys. **133**, 024701 (2010).
[30] V. I. Anisimov, J. Zaanen, and O. K. Andersen, Phys. Rev. B **44**, 943 (1991).
[31] S. L. Dudarev, G. A. Botton, S. Y. Savrasov, C. J. Humphreys, and A. P. Sutton, Phys. Rev. B **57**, 1505 (1998).
[32] D. Prezzi, D. Eom, K. T. Rim, H. Zhou, S. Xiao, C. Nuckolls, T. F. Heinz, G. W. Flynn, and M. S. Hybertsen, ACS Nano **8**, 5765 (2014).
[33] V. M. Karpan, P. A. Khomyakov, A. A. Starikov, G. Giovannetti, M. Zwierzycki, M. Talanana, G. Brocks, J. van den Brink, and P. J. Kelly, Phys. Rev. B **78**, 195419 (2008).
[34] See Supplemental Material at http://link.aps.org/supplemental/10.1103/PhysRevB.93.220406 for details related to the structures and binding energies for the 2D materials adsorbed on Co(111).
[35] See *Magnetic Properties of Metals: 3d, 4d and 5d Elements, Alloys and Compounds*, edited by H. P. J. Wijn, Landolt-Börnstein, New Series, Group III, Vol. 19, Pt. A (Springer, Berlin, 1986).
[36] M. Dion, H. Rydberg, E. Schröder, D. C. Langreth, and B. I. Lundqvist, Phys. Rev. Lett. **92**, 246401 (2004).
[37] K. Lee, E. D. Murray, L. Kong, B. I. Lundqvist, and D. C. Langreth, Phys. Rev. B **82**, 081101(R) (2010).
[38] J. Klimeš, D. R. Bowler, and A. Michaelides, J. Phys.: Condens. Matter **22**, 022201 (2010).
[39] J. Klimeš, D. R. Bowler, and A. Michaelides, Phys. Rev. B **83**, 195131 (2011).
[40] I. Hamada, Phys. Rev. B **89**, 121103(R) (2014).
[41] We have confirmed the validity of this approach from calculations on bulk fcc Co where we got reasonable agreement of the computed lattice constant (3.524 Å) with the experimental value (3.545 Å) [35].
[42] M. Corral Valero and P. Raybaud, J. Phys. Chem. C **118**, 22479 (2014).
[43] We note that the moment of the second and third Co layer is already close to the bulk value of $1.86\mu_B$.
[44] From this bulk coupling constant the mean-field Curie temperature T_C^{MF} can be estimated via $k_B T_C^{MF} = J_0/3$ [45,46], where here $J_0 = 12J_{bulk}$ is an effective exchange parameter [52] and k_B is the Boltzmann constant. Using this procedure, a value of $T_C^{MF} = 1132$ K is obtained, which is in reasonable agreement with previous values considering that only nearest-neighbor couplings are taken into account [45,46].
[45] M. Lezaic, P. Mavropoulos, and S. Blügel, Appl. Phys. Lett. **90**, 082504 (2007).
[46] We note that our exchange coupling constant is defined as twice the value compared to Ref. [45].
[47] J. E. Bickel, F. Meier, J. Brede, A. Kubetzka, K. von Bergmann, and R. Wiesendanger, Phys. Rev. B **84**, 054454 (2011).
[48] The calculated exchange coupling constants for the graphene/Fe/Ir(111) are $J_{fcc} = 31.7$ meV, $J_{hcp} = 30.3$ meV at the chemisorbed regions and $J_{top} = 13.5$ meV at the physisorbed sites.
[49] J. Brede, N. Atodiresei, S. Kuck, P. Lazić, V. Caciuc, Y. Morikawa, G. Hoffmann, S. Blügel, and R. Wiesendanger, Phys. Rev. Lett. **105**, 047204 (2010).
[50] N. Atodiresei, J. Brede, P. Lazić, V. Caciuc, G. Hoffmann, R. Wiesendanger, and S. Blügel, Phys. Rev. Lett. **105**, 066601 (2010).
[51] B. Dlubak, M.-B. Martin, R. S. Weatherup, H. Yang, C. Deranlot, R. Blume, R. Schloegl, A. Fert, A. Anane, S. Hofmann, P. Seneor, and J. Robertson, ACS Nano **6**, 10930 (2012).
[52] A. I. Liechtenstein, M. I. Katsnelson, V. P. Antropov, and V. A. Gubanov, J. Magn. Magn. Mater. **67**, 65 (1987).